HHS Public Access

Author manuscript

Cancer Res. Author manuscript; available in PMC 2019 August 01.

Published in final edited form as:

Cancer Res. 2018 August 01; 78(15): 4386–4395. doi:10.1158/0008-5472.CAN-18-0814.

Specific Targeting of *MTAP*-deleted Tumors with a Combination of 2′-Fluoroadenine and 5′-Methylthioadenosine

Baiqing Tang[1], **Hyung-Ok Lee**[1], **Serim S. An**[1], **Kathy Q. Cai**[1], and **Warren D. Kruger**[1,*]

[1]Cancer Biology Program, Fox Chase Cancer Center, Philadelphia, PA 19111

Abstract

Homozygous deletion of the methylthioadenosine phosphorylase (*MTAP*) gene is a frequent event in a wide variety of human cancers and is a possible molecular target for therapy. One potential therapeutic strategy to target *MTAP*-deleted tumors involves combining toxic purine analogs such as 6′-thioguanine (6TG) or 2′-fluoroadenine (2FA) with the MTAP substrate 5′-deoxy-5′-methylthioadenosine (MTA). The rationale is that excess MTA will protect normal *MTAP*$^{+}$ cells from purine analog toxicity because MTAP catalyzes the conversion of MTA to adenine, which then inhibits the conversion of purine base analogs into nucleotides. However, in *MTAP*$^{-}$ tumor cells, no protection takes place because adenine is not formed. Here, we examine the effects of 6TG and 2FA in combination with MTA *in vitro* and *in vivo*. *In vitro*, MTA protected against both 6TG and 2FA toxicity in an *MTAP*-dependent manner, shifting the IC_{50} concentration by one to three orders of magnitude. However, in mice, MTA protected against toxicity from 2FA but failed to protect against 6TG. Addition of 100 mg/kg MTA to 20 mg/kg 2FA entirely reversed the toxicity of 2FA in a variety of tissues and the treatment was well tolerated by mice. The 2FA +MTA combination inhibited tumor growth of four different *MTAP*$^{-}$ human tumor cell lines in mouse xenograft models. Our results suggest that 2FA+MTA may be a promising combination for treating *MTAP*-deleted tumors.

Keywords

purine analog; methionine; metabolism; chemotherapy; mouse

Introduction

A quarter century ago, Toohey first recognized that certain murine malignant hematopoietic cell lines lacked MTAP activity (1). MTAP is a key enzyme in the purine and methionine salvage pathways that catalyzes the conversion of the polyamine byproduct MTA into the purine base adenine and the sugar methylthioribose-1-phosphate. MTAP is ubiquitously expressed at high levels in all tissues in the human body. The gene encoding human *MTAP* is located on chromosome 9p21, about 80 kb toward the telomere from the *CDKN2A/ARF* region (2, 3). Homozygous deletion of *MTAP* is frequent in a large number of different

*Correspondence: Warren Kruger, Fox Chase Cancer Center, 333 Cottman Ave., Philadelphia PA, 19111 Phone: 215-728-3030 Fax: 215-214-1623. warren.kruger@fccc.edu.

Disclosure of Potential Conflicts of Interest: No potential conflicts of interest were disclosed.

human cancers including leukemia, lymphoma, lung, pancreas, squamous cell, billiary tract, brain, bone, breast, prostate, bladder, mesothelioma, endometrial, melanoma, gastrointestinal, and neuroendocrine (4–28). It is also important to note that deep sequencing suggests that homozygous deletion of the 9p21 region appears to be an early event in tumor evolution (29), and immunohistochemical staining for MTAP also suggests a distinct lack of heterogeneity (10, 30, 31). Taken together, these findings suggest that a therapy that specifically targets *MTAP*$^{-}$ cells could be useful in treating a wide variety of different types of cancer. Recently, three different groups have performed synthetic lethal screens and discovered that *MTAP*$^{-}$ cells are more sensitive to down regulation of protein arginine N-methyltransferase 5 (PRMT5) (32–34). However, when pharmacologic inhibitors of PRMT5 were used, they seemed to inhibit cell growth with either no (34) or little relationship to MTAP status (32). In addition, since PRMT5 is essential for cell viability, it is unclear if pharmacologic inhibition of PRMT5 can be used without significant side effects.

Here, we explore a different strategy to target *MTAP*$^{-}$ cells involving a combination of purine analogs and MTA. Purine analogs (PAs), such as mercaptopurine or 6-thioguanine, are among the oldest chemotherapy agents (35). These analogs are actually prodrugs, which must be converted to nucleotides in order to be active. This process occurs through the action of specific phosphoribosyl transferase enzymes that transfer a ribose and phosphate from phosphoribosylpyrophosphate (PRPP) to the base. Once activated, these drugs interfere with DNA replication and cellular metabolism by inhibiting enzymes that normally bind nucleotides. The major limitation with this class of drugs is that they target all dividing cells, not just cancer cells. At a clinical level, this means the physician has a limited “therapeutic window” in which to use these drugs, balancing the killing of tumor cells with the toxicity to the patient. In theory, if the effect of these agents on normal tissue could be ameliorated, much higher doses could be used and this would likely increase their clinical effectiveness.

One way to protect cells from the toxicity of purine analogs is to prevent their conversion to nucleotides by competition for PRPP (Fig. 1). When MTA is combined with purine analogs in the presence of MTAP, excess MTA is converted to adenine, which is then reacted with PRPP to make adenosine 5′-monophosphate (AMP). This reaction is catalyzed by adenine phosphoribosyltransferase (APRT). Thus, in the presence of high concentrations of MTA, PRPP levels may become depleted and PAs cannot not be converted to 5′-monophosphate form of the purine analog (PAMP). However, in tumor cells lacking MTAP, no excess adenine is produced, resulting in increased production of PAMP and increased cell death.

Previously published work by two different groups shows that this general strategy works well in cell culture (36, 37). However, the key question of whether MTA can protect against PA toxicity *in vivo* has not been definitively explored. There are two reports in the literature suggesting that MTA can protect against 6TG toxicity in mice, but these studies have involved very few animals and are not well described (20, 38). Here, we have performed a series of experiments examining the ability of MTA to protect against toxicity to two different purine analogs, 6TG and 2FA. Surprisingly, while we see excellent MTAP/MTA-mediated protection of both compounds in cell culture, we only see MTAP/MTA-mediated protection for 2FA in mice. Furthermore, the combination of 2FA and MTA inhibits tumor

growth in several different *MTAP*$^{-}$ xenograft models. Our findings suggest that 2FA+MTA may be useful in the treatment of *MTAP*$^{-}$ cancers.

Materials and Methods

Chemicals and drug preparation

For cell culture studies, 6TG (Sigma), 2FA (Oakwood Chemical), and MTA (Sigma) were dissolved directly in cell culture medium. For mouse studies, 6TG was dissolved at a concentration of 2.7 mg/ml in 1% carboxymethylcellulose (Sigma) in filter-sterilized water. For 6TG/MTA, MTA was added to the 6TG carboxymethylcellulose solution at a concentration of 3.6 mg/ml. 2FA was dissolved at a concentration of 0.36 mg/ml in the presence of equal normality sulfuric acid in a 1% carboxymethylcellulose solution. MTA was added to the 2FA solution at a concentration of 1.8 mg/ml.

Cell lines

Cell lines, along with MTAP status, used for this study are listed in Supplementary Tables 1 and 2. All cell lines were originally obtained either from the ATCC or were created in the Fox Chase Cancer Center Cell Culture Facility and have been previously described (37), with the exception of the NIH3T3 cells that have had MTAP inactivated by CRISPR (see below). Cells were grown in 2 mM glutamine, 100 μg/ml penicillin, 100 μg/ml streptomycin, 10% fetal bovine serum (FBS), and 250 μg/ml G418 for no more than 5 passages after thaw. Cells are tested for mycoplasma at the time of thaw. No cell line authentication was performed by our lab.

We generated *Mtap* deletion in NIH3T3 cells by CRISPR/Cas9 using a method in Bauer *et. al.* (2015). Two sets of sgRNAs were designed to delete *Mtap* exons 5 and 6 (sgRNA-A: CACCGGGCAAAACGGTTCAGCCAT, sgRNA-A-rc: AAACATGGCTGAACCGTTTTGCCC, sgRNA-B: CACCGTTTCCTTTGCATTTGTCTCG, sgRNA-B-rc: AAACCGAGACAAATGCAAAGGAAAC). For CRISPR cloning, phosphorylated oligos were ligated into Bbs 1 site of eSpCas9 (1.1)-1 vector and transformed into DH5α cells. Colonies were verified by sequence using U6 promoter primer (CGTAACTTGAAAGTATTTCGATTTCTTGGC). Each CRISPR pair was co-transfected with GFP expression plasmid (pAcGFP1-N1) into NIH3T3 cells by electroporation using Amax Cell Line Nucleofactor Kit R (Lonza). Top ~3% of GFP positive cells were sorted by FACS (Fluorescence Activated Cell Sorting) and plated individually to grow clone. Genomic DNAs from parental and sorted cells were isolated and validated *Mtap* deletion by PCR (Qiagen HotStar Taq Master Kit) using deletion screening primers (MTAP del-F: GTCTTTGGAGGGACAGCAAG and MTAP del-R: ACCCATGTGGCGTAAGAGTC). Selected clones were further evaluated for *Mtap* deletion by sequencing and MTAP activity.

IC_{50} studies

For IC_{50} studies cells were plated out at a density of 3,000 cells per well in a 96-well cell culture plate. Wells were exposed to either nothing or drug at 2-fold increasing concentrations over a 128-fold range. Each dose was tested in triplicate. Plates were

incubated for 48 hours. Growth was measured by MTT assay (Cell Titer 96, Promega). IC_{50} values were then calculated using GraphPad Prism 5.0 software.

Mixing experiment using CRISPR MTAPΔ cells

Parental NIH3T3 cells and CRISPR MTAPΔ cells were mixed either 1:1 or 4:1 ratio and then treated with either none or 2FA (1.25 μM)+ MTA (10 μM). After 70 hours of incubation, cells were harvested and extracted genomic DNAs were performed allele specific PCR using specific primers either for wild-type MTAP (GTCTTTGGAGGGACAGCAAG and CACACATTCAGGTCCACTGC, 300 bp PCR product) or for MTAPΔ allele detection (TGCCAGAGGATCGGGGCCTTG and ACCCATGTGGCGTAAGAGTC, 706 bp PCR product).

Mouse toxicity studies

Mouse toxicity studies were performed using C57BL6 animals and were approved by the Fox Chase Cancer Center IACUC. Mice were injected i.p. with the dose and frequency as indicated in figure legends, with the exception of Supplementary Fig. 3 (oral gavage) and Supplementary Fig. 5 (osmotic pump). For blood analysis, samples were taken by retro orbital bleed and complete blood counts were performed using an Abaxis Vetscan5. At the end of experiments, mice were euthanized and liver, spleen, thymus, colon and bone marrow were collected, fixed in buffered formalin and embedded in paraffin. The paraffin blocks were cut into 5-μm-thick sections that were placed on positively charged slides. Sections were stained with hematoxylin and eosin (HE) and mounted with Permount (Fischer Scientific, Pittsburgh, PA). All HE slides were viewed with a Nikon Eclipse 50i microscope and photomicrographs were taken with an attached Nikon DS-Fi1 camera (Melville, NY, USA).

For Caspase 3 and Ki67 immunohistochemical staining, 5-μm formalin-fixed, paraffin embedded sections were deparaffinized, hydrated, and subjected to heat-induced epitope retrieval with 0.01 M citrate buffer (pH 6.0). Endogenous peroxidases were quenched by the immersion of slides in 3% hydrogen peroxide solution. Sections were incubated overnight with primary antibodies to anti-human ki-67 (1:100, Cat No. M7240, DAKO) and cleaved caspase-3 (1:200, Cat No. 9661 Cell Signaling) at 4 °C in a humidified slide chamber. Immonodetection was performed using the Dako Envision+ polymer system and immunostaining was visualized with the chromogen 3, 3’-diaminobenzidine. The sections were then washed, counterstained with hematoxylin, dehydrated with ethanol series, cleared in xylene, and mounted. As a negative control, the primary antibody was replaced with normal mouse/rabbit IgG to confirm absence of specific staining. Image analysis quantiation was performed by scanning with an Aperio ScanScope CS 5 slide scanner (Aperio, Vista, CA, USA). Scanned images were then viewed with Aperio's image viewer software (ImageScope, version 11.1.2.760, Aperio). Selected regions of interest were outlined manually by a pathologist (K.Q.).

Mouse xenograft studies

C.B17 SCID mice were injected in the hind flank with 1×10^7 of tumor cells in 200 μl of matrigel. Tumors were then allowed to grow until visible (1–4 weeks depending on line) and

mice were randomly divided into vehicle and treatment groups. Mice were then treated with either vehicle or drug combination at a schedule indicated in figures. Tumor size was measured weekly by calipers as described (39) in all experiments except for Fig. 7a in which tumor volume was measured by MRI (40). Tumor growth was calculated by comparing the difference in volume at T_n with the volume at the time of the start of treatment (T_0).

Statistics

Pairwise comparisons between groups were performed using a Student's two-sided t-test. A p-value of 0.05 or less was considered significant. For multiple group comparisons single sided ANOVA was used followed by post-hoc test. All graphs show standard error of mean (SEM).

Results

MTA protects against 6TG toxicity *in vitro*, but not *in vivo*

We examined the effects of MTA addition on 6TG cell killing in a variety of $MTAP^+$ and $MTAP^-$ cell lines. For each line, we determined the IC_{50} of 6TG at 48 hours in the presence or absence of 10 μM MTA and compared the ratio of the IC_{50} concentrations. In $MTAP^+$ cells, we observed a 360-fold mean increase in IC_{50} concentration when MTA was added, but in $MTAP^-$ cells the mean increase was only two fold (Supplementary Fig. 1A, Supplementary Table 1). These findings confirm that MTA protects $MTAP^+$ cells significantly better than $MTAP^-$ cells from 6TG toxicity.

We next performed a series of *in vivo* experiments comparing the effects of 6TG alone versus 6TG+MTA. We injected (i.p.) C57BL6 mice with a single dose of either vehicle, 6TG (75 mg/kg), a combination of 6TG (75 mg/kg) + MTA (100 mg/kg), or a combination 6TG (75 mg/kg) + adenine (45 mg/kg). After four days, we examined toxicity by assessing white blood cell counts. As expected, mice treated with 6TG showed significantly reduced numbers white blood cells, lymphocytes, and neutrophils compared to untreated control animals (Supplementary Fig. 1B). However, we observed no beneficial effect of the addition of MTA or adenine. This result was surprising to us especially given the report by Bertino et al. that MTA could alleviate the lethality caused by multiple 6TG injections in SCID mice (38). Therefore, we performed an identical experiment in which we gave either SCID mice or C57BL6 mice, 6TG (75 mg/kg) or 6TG (75 mg/kg)+ MTA (100mg/kg) using the same schedule reported in their paper and followed the animals over time. In our hands, all of the animals in both groups died by 24 days from the start of treatment, and there was no difference between the non-MTA treated and the MTA treated animals (Supplementary Fig. 1C, Supplementary Fig. 2). A series of additional experiments were also performed in which we varied the mouse route of administration (oral and infusion pump), the timing of the MTA relative to the 6TG administration, and changed the ratio of 6TG to MTA (Supplementary Fig. 3–6). None of the experiments showed any evidence that MTA could alleviate 6TG toxicity.

Lastly, we performed a tissue toxicity study where the animals were injected with either vehicle, 6TG, or 6TG + MTA for four consecutive days. On the fifth day, the animals were

euthanized and the intestine, spleen, bone marrow and thymus were collected and analyzed for histopathology, and blood was collected for white blood cell analysis. Mice treated with 6TG exhibited the most severe toxicity in intestine and bone marrow (Supplementary Fig. 7A and B). The intestine showed severe mucosal atrophy, infiltration of inflammatory cells, and the basal portions of the glands were dilated. Bone marrow exhibited a dramatic decrease in cellularity. More modest atrophy was observed in the spleen and thymus. In blood, we observed a 40% decrease in white blood cells (p=0.002), a 36% decrease in lymphocytes (P=0.0017), and a 69% decrease in neutrophils (P=0.0005) (Supplementary Fig. 7C). Addition of MTA did not appear to significantly reverse toxicity in any of the tissues examined and actually made the neutropenia worse. Our experiments taken together show that MTA is unable to protect tissues against 6TG toxicity *in vivo*.

MTA protects against 2FA toxicity in an *MTAP*-dependent manner in cell culture

Our inability to ameliorate 6-TG toxicity by MTA or adenine *in vivo* was puzzling to us, especially given the robust protection we always observed in *MTAP*$^{+}$ cells *in vitro*. One possible explanation is that *in vivo* PRPP is not rate limiting, so even in the presence of adenine, there is sufficient PRPP to facilitate the conversion to 6TG to 6TGMP. If this was the case using a direct adenine analog might bypass this problem as adenine and the adenine analog would compete directly for binding to the APRT enzyme. To examine this possibility, we chose to examine 2FA, as fludarabine (2FA attached to a modified sugar-phosphate moiety) is used clinically to treat certain types of cancers (41). Interestingly, 2FA has never been tested in humans because early animal studies suggested it would be too toxic (42).

Our first series of experiments were cell line studies to determine if MTA could protect against killing by 2FA *in vitro*. Initially we examined the effects using an isogenic *MTAP*$^{+}$ and *MTAP*$^{-}$ cell line derived from a human HT1080 fibrosarcoma cell line previously developed in the lab (37). In *MTAP*$^{-}$ cells, a 48-hour exposure to 2FA effectively killed all cells with a calculated IC_{50} of 75 nM (Fig. 2A). The addition of 10 μM MTA did not affect the IC_{50}, whether added at the same time, one, or two hours before 2FA exposure. In contrast, in *MTAP*$^{+}$ cells, addition of MTA dramatically increased the IC_{50} from 27 nM to 663 nM. We also tested the effects of 2FA +/− MTA on an isogenic set of *MTAP*$^{+}$ and *MTAP*$^{-}$ non-transformed mouse NIH 3T3 cells made by deleting MTAP using CRISPR. Again we saw a dramatic shift in IC_{50} concentrations when MTA was added to 2FA only when MTAP was present (Fig. 2B). In addition to these isogenic cell lines, we also examined a number of other *MTAP*$^{+}$ and *MTAP*$^{-}$ cell lines for MTA protection. On average, we observed a 21-fold increase in the IC_{50} concentration in *MTAP*$^{+}$ cells, but no significant change in *MTAP*$^{-}$ cells (Fig. 2C; Supplementary Table 2). These studies suggest that MTA can protect against the effects of 2FA toxicity in cell lines similar to that observed for 6TG.

We also performed a mixing experiment designed to determine if *MTAP*$^{+}$ cells could protect *MTAP*$^{-}$ cells from 2FA+MTA toxicity *in trans*. We mixed wild-type and CRISPR *MTAP*-deleted NIH3T3 cells in either a 1:1 or 4:1 ratio and then treated them with either nothing or 2FA+MTA. After 70 hours, cells were harvested and allele specific PCR was performed to determine the relative abundance of the *MTAP*$^{+}$ and MTAP-deleted allele (Fig. 2D). After 2FA+MTA treatment, we are unable to detect the PCR product from the MTAP-deleted

allele, but see a strong band for the *MTAP*$^{+}$ allele. These results indicate that *MTAP*$^{+}$ cells do not protect *MTAP*$^{-}$ cells from killing by 2FA+MTA *in trans*.

MTA protects against 2FA toxicity in mice

Some limited toxicology studies have been performed in mice for 2FA (see toxnet.nlm.nih.gov) showing that the LD_{50} for 2FA in mice (11.34 mg/kg) is significantly lower than the LD_{50} for 6TG (54 mg/kg). Based on this information, we performed an initial experiment in which C57BL6 mice were given 2FA at either 5 and 20 mg/kg in the presence or absence of MTA (100 mg/kg). Mice were given the drugs by ip injection once a day for five days and then blood was analyzed eight days after the final injection (Fig. 3A). All of the animals survived to this time, and blood counts revealed that the 20 mg/kg 2FA dose caused a significant reduction in white blood cells and lymphocytes. Importantly, the mice treated with a combination of 2FA (20 mg/kg) + MTA (100 mg/kg) had lymphocyte counts indistinguishable from the control animals. Based on this result, we performed a follow up study in which we obtained blood and weighed each animal both before and after treatment (Fig 3B and C). In mice treated with 2FA alone lymphocytes counts decreased 70.2% ($p<0.0003$) after treatment but in animals treated with the 2FA+MTA combination the decrease was only 21.4% ($p<0.04$). In addition, while mice treated with 2FA alone lost on average 4.2 grams of weight ($p<0.009$), mice receiving 2FA+MTA only lost 0.3 grams.

We next examined the effects of 2FA (20 mg/kg) and 2FA (20 mg/kg) + MTA (100 mg/kg) on mouse tissues using a protocol identical to that used for 6TG. 2FA alone caused significant toxicity to all four tissues examined: small intestine, bone marrow, spleen and thymus (Fig. 4A). Compared to 6TG, 2FA caused significantly more toxicity in small intestine, spleen, and thymus, but was somewhat less toxic with regards to bone marrow (Fig. 4B). In terms of blood cells, 2FA treated mice exhibited greater lymphopenia, but did not exhibit neutropenia (Fig. 4C). Strikingly, addition of MTA to 2FA almost entirely prevented all the toxic effects of 2FA. Intestine, bone marrow, spleen, and thymus treated with the 2FA+MTA were all indistinguishable from untreated control samples. In this experiment, white blood cell and lymphocyte counts in 2FA+MTA were not statistically different from control animals. We also performed an additional study in which mice were injected with either 2FA (20 mg/kg), or 2FA (20 mg/kg) + MTA (100 mg/kg) for eight times over a ten day period and then monitored for survival an additional 22 days. While all of the 2FA alone animals died by day 16, all of the 2FA+MTA animals were alive at day 28 (Supplementary Fig. 8). Together, these studies show that MTA can protect against 2FA related toxicity *in vivo*.

Xenograft studies

We next examined the effectiveness of 2FA+MTA in inhibiting human *MTAP*$^{-}$ tumor cell growth in SCID mice. For these studies, we used 10mg/kg 2FA and 50 mg/kg MTA, as we found that SCID mice were somewhat less tolerant of the combination (Supplementary Fig. 9A,B). In our first study, we injected 1×10^{7} *MTAP*$^{-}$ HT1080 cells subcutaneously and allowed to form palpable tumors. Mice were then randomly divided and injected with either 2FA+MTA or vehicle alone (Fig. 5A). After 15 days, we observed a statistically significant decrease in tumor growth in the treated compared to the untreated mice. To show that tumor

growth inhibition was dependent on loss of *MTAP*, we performed a second experiment in which we compared the response of isogenic *MTAP*$^{-}$ and *MTAP*$^{+}$ HT1080 cells to 2FA +MTA (Fig. 5B). We observed that in mice treated with 2FA+MTA, the relative growth rate of *MTAP*$^{-}$ tumors was significantly slower than that observed for *MTAP*$^{+}$ tumors. At the end of the experiment, tumors were excised and analyzed for MTAP activity, Ki67 staining, and Caspase 3 staining. As expected, high levels of MTAP activity were detected only in the tumors formed by the *MTAP*$^{+}$ cells (Fig 5C). We found no difference in Ki67 staining, but saw a significant increase in the fraction of cell staining positive for Caspase 3, suggesting that 2FA+MTA is stimulating apoptosis (Fig. 6).

We tested three additional *MTAP*$^{-}$ tumor cell lines for growth inhibition by 2FA+MTA in SCID mice. A172 and U87 cells are glioblastoma-derived lines, while A549 cells are derived from a lung adenocarcinoma. Both tumor types show high rates of *MTAP*-loss. In mice containing U87 and A549 xenografts, we observed significant tumor growth inhibition in 2FA+MTA treated mice compared to vehicle treated mice (Fig. 7A and B). In mice bearing A172 xenograft tumors, treatment with 2FA+MTA resulted in a dramatic shrinkage of the tumors (Fig. 7C). These studies indicate that 2FA+MTA can inhibit the growth of a variety of MTAP-deleted tumor xenografts.

In the U87 xenograft experiment, in which the animals received a total of 15 injections over a 36-day period, we also measured the weight of the animals (Fig. 7D). Mice initially lost about 15% of their body weight during the first week of treatment with 2FA+MTA, but after the first week they started to gain weight at a rate that was similar to that observed in vehicle-treated animals. These data suggest that the 2FA+MTA combination can be given relatively frequently and for long duration without adverse effects.

Discussion

In this paper, we explore two different drug combinations, 6TG+MTA and 2FA+MTA, for their potential as agents to treat tumors that lack expression of MTAP. The underlying concept is that MTA will act as a “protecting agent” in cells that express MTAP, but will not protect in tumor cells lacking MTAP expression. This protection occurs because MTAP converts MTA to adenine, which is then converted to AMP by addition of a sugar and phosphate moiety that comes from PRPP. Since 6TG and 2FA both require conversion to either 6TGMP or 2FAMP to be toxic, it is hypothesized that the presence of high concentrations of adenine will reduce the PRPP pool, resulting in a reduction in the formation 6TGMP and 2FAMP. In cell culture, this mechanism is likely to be correct. Lubin found that addition of MTA to *MTAP*$^{+}$ human fibroblasts cells protected these cells from the toxic effects of 2,6-diaminopurine, 6-methylpurine and 2FA, but addition of MTA did not protect *MTAP*$^{-}$ tumor cells (36). Using a pair of genetically engineered isogenic *MTAP*$^{+}$ and *MTAP*$^{-}$ cell lines, our lab previously showed that addition of MTA shifted the IC_{50} of 6TG from 0.19 μM to 3.7 μM in *MTAP*$^{+}$ cells, but did not shift the IC_{50} in *MTAP*$^{-}$ cells (37). However, when adenine was added, both *MTAP*$^{+}$ and *MTAP*$^{-}$ cells were protected. Additionally, treatment with a pharmacologic inhibitor of MTAP entirely abolished protection by MTA. In this manuscript, we show that MTA can protect against 2FA toxicity to a similar extent.

The surprising finding from the mouse studies reported here was that while MTA protected against 2FA toxicity, it failed to protect against 6TG toxicity. We first focused on the 6TG +MTA combination because 6TG was already an FDA approved drug and the two reports in the literature suggested that MTA could protect against 6TG toxicity (20, 38). Despite varying the amount of 6TG used, the ratio of MTA to 6TG, and the mode of delivery, we failed to see significant levels of protection by MTA. Toxicity in these studies was examined in a variety of assays including white blood cell counts, histopathology of various tissues, and survival. It should be noted that even when we used the identical concentrations of 6TG and MTA reported in the two previous reports, the exact same schedule, the same method of delivery, and the same outcome measure (survival), we were unable to repeat their observations. We have no explanation for this difference in results, although it is possible that there were subtle differences in the mouse strains that were used (C.B17 SCID vs. NOD SCID) or the timing of the administration of 6TG and MTA.

However, we did observe robust *in vivo* protection with the combination of 2FA and MTA. Treatment of C57BL6 mice with 20 mg/kg 2FA by itself resulted in severe toxicity in the small intestine, spleen, thymus, and moderate toxicity in the bone marrow. This pattern of toxicity was somewhat different from that observed with 75 mg/kg 6TG, which was particularly hard on the bone marrow, but not as severe on the other tissues. Amazingly, the addition 100 mg/kg MTA to 2FA almost completely eliminated the toxic effects. For the most part, tissues of mice treated with the 2FA+MTA combination were indistinguishable from control animals. Mice tolerated multiple injections quite well, and maintained weight while on treatment. An interesting question is: Why did MTA protect against both 6TG and 2FA toxicity *in vitro*, but only 2FA *in vivo*? A possible explanation may be related to differences in what is rate-limiting in the mechanism of activation of the two drugs. In cell culture, it is likely that PRPP depletion by MTA is the critical component. Both 2FA and 6TG require PRPP for transformation into their respective nucleotide analogs and the absolute concentration of MTA added to the cell culture medium is high (10 μM), thus PRPP depletion seems quite likely. However, *in vivo* it is unlikely that we are achieving these very high MTA levels, and even if we were, it is unknown if PRPP concentrations in tissues are similar to what is observed in cell culture. The fact that addition of adenine did not protect against 6TG toxicity (Fig. 2B) also strongly suggests that depletion of PRPP is not occurring *in vivo*. The most likely reason MTA protects against 2FA is that adenine and 2FA compete directly for binding to APRT and thus prevents the formation of 2FAMP. In contrast because 6TG uses GPRT for activation (43), there would be no direct completion between 6TG and adenine.

We used the combination of 2FA+MTA to examine growth inhibition of four different MTAP-deleted tumor cell lines in SCID mice as xenografts. In all cases, we found that treatment of mice with 2FA+MTA inhibited tumor growth compared to vehicle treated controls. We also used isogenic HT1080 cell lines that were either $MTAP^{+}$ or $MTAP^{-}$ to examine the effect of *MTAP* status on treatment. As expected, we found that the 2FA+MTA combination was much more effective in inhibiting the growth of $MTAP^{-}$ tumor cells than $MTAP^{+}$ cells. We also observed a significantly higher percentage of cells from $MTAP^{-}$ tumors that were positive for the apoptotic marker Caspase 3, but observed no difference in the cell cycle marker, Ki67. This finding may explain why, with one exception, we only

observed a slowing of tumor growth and not regression of tumors in the mouse xenografts. We hypothesize that in fast growing xenograft tumors the division rate is much faster than the apoptotic rate. Consistent with this idea, we observed regression in A172 cells, which also had the slowest growth rate.

While the results reported here are encouraging, there are many additional studies that will need to be performed before human clinical trials can begin. For all of the experiments reported here, we used a five to one ratio of MTA to 2FA and we have not explored other ratios. In addition, our use of 20 mg/kg 2FA and 100 mg/kg MTA was the maximum we could use given the solubility of these two compounds. Higher doses might be achievable by either optimizing solvent choice or by giving the compounds orally instead of by injection. It seems reasonable to assume that the higher the dose of 2FA that could be delivered, the more effective the treatment would be. Lastly, pharmacodynamics studies will need to be performed to optimize drug dosing and delivery.

In summary, we show here that the combination of 2FA+MTA has potential as an agent to specifically target human tumors lacking expression of *MTAP*. Given the high frequency of *MTAP* loss in a variety of tumor types, we believe this combination is worth pursuing.

Supplementary Material

Refer to Web version on PubMed Central for supplementary material.

Acknowledgments

We acknowledge the help the Fox Chase Laboratory Animal, Biological Imaging, and Experimental Histopathology Facilities. We also acknowledge critical reviewing of the manuscript by Sapna Gupta. Some funding for these studies came from the Fox Chase Cancer Center core grant, NIH CA006927.

References

1. Toohey JI. Methylthioadenosine nucleoside phosphorylase deficiency in methylthio-dependent cancer cells. Biochem Biophys Res Commun. 1978; 83:27–35. [PubMed: 100109]
2. Carrera CJ, Eddy RL, Shows TB, Carson DA. Assignment of the gene for methylthioadenosine phosphorylase to human chromosome 9 by mouse-human somatic cell hybridization. Proc Natl Acad Sci U S A. 1984; 81:2665–8. [PubMed: 6425836]
3. Olopade OI, Bohlander SK, Pomykala H, Maltepe E, Van Melle E, Le Beau MM, et al. Mapping of the shortest region of overlap of deletions of the short arm of chromosome 9 associated with human neoplasia. Genomics. 1992; 14:437–43. [PubMed: 1385305]
4. Batova A, Diccianni MB, Nobori T, Vu T, Yu J, Bridgeman L, et al. Frequent deletion in the methylthioadenosine phosphorylase gene in T- cell acute lymphoblastic leukemia: strategies for enzyme-targeted therapy. Blood. 1996; 88:3083–90. [PubMed: 8874207]
5. Hori Y, Hori H, Yamada Y, Carrera CJ, Tomonaga M, Kamihira S, et al. The methylthioadenosine phosphorylase gene is frequently co-deleted with the p16INK4a gene in acute type adult T-cell leukemia. Int J Cancer. 1998; 75:51–6. [PubMed: 9426690]
6. Dreyling MH, Roulston D, Bohlander SK, Vardiman J, Olopade OI. Codeletion of CDKN2 and MTAP genes in a subset of non-Hodgkin's lymphoma may be associated with histologic transformation from low- grade to diffuse large-cell lymphoma. Genes Chromosomes Cancer. 1998; 22:72–8. [PubMed: 9591637]

7. Bertino JR, Lubin M, Johnson-Farley N, Chan WC, Goodell L, Bhagavathi S. Lack of expression of MTAP in uncommon T-cell lymphomas. Clin Lymphoma Myeloma Leuk. 2012; 12:306–9. [PubMed: 23040436]
8. Usvasalo A, Ninomiya S, Raty R, Hollmen J, Saarinen-Pihkala UM, Elonen E, et al. Focal 9p instability in hematologic neoplasias revealed by comparative genomic hybridization and single-nucleotide polymorphism microarray analyses. Genes Chromosomes Cancer. 2010; 49:309–18. [PubMed: 20013897]
9. Schmid M, Malicki D, Nobori T, Rosenbach MD, Campbell K, Carson DA, et al. Homozygous deletions of methylthioadenosine phosphorylase (MTAP) are more frequent than p16INK4A (CDKN2) homozygous deletions in primary non-small cell lung cancers (NSCLC). Oncogene. 1998; 17:2669–75. [PubMed: 9840931]
10. Watanabe F, Takao M, Inoue K, Nishioka J, Nobori T, Shiraishi T, et al. Immunohistochemical diagnosis of methylthioadenosine phosphorylase (MTAP) deficiency in non-small cell lung carcinoma. Lung Cancer. 2009; 63:39–44. [PubMed: 18555557]
11. Subhi AL, Tang B, Balsara BR, Altomare DA, Testa JR, Cooper HS, et al. Loss of methylthioadenosine phosphorylase and elevated ornithine decarboxylase is common in pancreatic cancer. Clin Cancer Res. 2004; 10:7290–6. [PubMed: 15534104]
12. Hustinx SR, Hruban RH, Leoni LM, Iacobuzio-Donahue C, Cameron JL, Yeo CJ, et al. Homozygous deletion of the MTAP gene in invasive adenocarcinoma of the pancreas and in periampullary cancer: a potential new target for therapy. Cancer Biol Ther. 2005; 4:83–6. [PubMed: 15662124]
13. Chen YJ, Lin SC, Kao T, Chang CS, Hong PS, Shieh TM, et al. Genome-wide profiling of oral squamous cell carcinoma. J Pathol. 2004; 204:326–32. [PubMed: 15372456]
14. Karikari CA, Mullendore M, Eshleman JR, Argani P, Leoni LM, Chattopadhyay S, et al. Homozygous deletions of methylthioadenosine phosphorylase in human biliary tract cancers. Mol Cancer Ther. 2005; 4:1860–6. [PubMed: 16373701]
15. Brat DJ, James CD, Jedlicka AE, Connolly DC, Chang E, Castellani RJ, et al. Molecular genetic alterations in radiation-induced astrocytomas. Am J Pathol. 1999; 154:1431–8. [PubMed: 10329596]
16. Suzuki T, Maruno M, Wada K, Kagawa N, Fujimoto Y, Hashimoto N, et al. Genetic analysis of human glioblastomas using a genomic microarray system. Brain Tumor Pathol. 2004; 21:27–34. [PubMed: 15696966]
17. Crespo I, Tao H, Nieto AB, Rebelo O, Domingues P, Vital AL, et al. Amplified and homozygously deleted genes in glioblastoma: impact on gene expression levels. PLoS One. 2012; 7:e46088. [PubMed: 23029397]
18. Garcia-Castellano JM, Villanueva A, Healey JH, Sowers R, Cordon-Cardo C, Huvos A, et al. Methylthioadenosine phosphorylase gene deletions are common in osteosarcoma. Clin Cancer Res. 2002; 8:782–7. [PubMed: 11895909]
19. Curtis C, Shah SP, Chin SF, Turashvili G, Rueda OM, Dunning MJ, et al. The genomic and transcriptomic architecture of 2,000 breast tumours reveals novel subgroups. Nature. 2012; 486:346–52. [PubMed: 22522925]
20. Collins CC, Volik SV, Lapuk AV, Wang Y, Gout PW, Wu C, et al. Next generation sequencing of prostate cancer from a patient identifies a deficiency of methylthioadenosine phosphorylase, an exploitable tumor target. Mol Cancer Ther. 2012; 11:775–83. [PubMed: 22252602]
21. Stadler WM, Olopade OI. The 9p21 region in bladder cancer cell lines: large homozygous deletion inactivate the CDKN2, CDKN2B and MTAP genes. Urol Res. 1996; 24:239–44. [PubMed: 8873383]
22. Illei PB, Rusch VW, Zakowski MF, Ladanyi M. Homozygous deletion of CDKN2A and codeletion of the methylthioadenosine phosphorylase gene in the majority of pleural mesotheliomas. Clin Cancer Res. 2003; 9:2108–13. [PubMed: 12796375]
23. Zimling ZG, Jorgensen A, Santoni-Rugiu E. The diagnostic value of immunohistochemically detected methylthioadenosine phosphorylase deficiency in malignant pleural mesotheliomas. Histopathology. 2012; 60:E96–105. [PubMed: 22394205]

24. Wong YF, Chung TK, Cheung TH, Nobori T, Chang AM. MTAP gene deletion in endometrial cancer. Gynecol Obstet Invest. 1998; 45:272–6. [PubMed: 9623796]
25. Meyer S, Fuchs TJ, Bosserhoff AK, Hofstadter F, Pauer A, Roth V, et al. A seven-marker signature and clinical outcome in malignant melanoma: a large-scale tissue-microarray study with two independent patient cohorts. PLoS One. 2012; 7:e38222. [PubMed: 22685558]
26. Powell EL, Leoni LM, Canto MI, Forastiere AA, Iocobuzio-Donahue CA, Wang JS, et al. Concordant loss of MTAP and p16/CDKN2A expression in gastroesophageal carcinogenesis: evidence of homozygous deletion in esophageal noninvasive precursor lesions and therapeutic implications. Am J Surg Pathol. 2005; 29:1497–504. [PubMed: 16224217]
27. Kim J, Kim MA, Min SY, Jee CD, Lee HE, Kim WH. Downregulation of methylthioadenosin phosphorylase by homozygous deletion in gastric carcinoma. Genes Chromosomes Cancer. 2011; 50:421–33. [PubMed: 21412930]
28. Huang HY, Li SH, Yu SC, Chou FF, Tzeng CC, Hu TH, et al. Homozygous deletion of MTAP gene as a poor prognosticator in gastrointestinal stromal tumors. Clin Cancer Res. 2009; 15:6963–72. [PubMed: 19887491]
29. Andor N, Graham TA, Jansen M, Xia LC, Aktipis CA, Petritsch C, et al. Pan-cancer analysis of the extent and consequences of intratumor heterogeneity. Nat Med. 2016; 22:105–13. [PubMed: 26618723]
30. Krasinskas AM, Bartlett DL, Cieply K, Dacic S. CDKN2A and MTAP deletions in peritoneal mesotheliomas are correlated with loss of p16 protein expression and poor survival. Mod Pathol. 2010; 23:531–8. [PubMed: 20081810]
31. He HL, Lee YE, Shiue YL, Lee SW, Chen TJ, Li CF. Characterization and Prognostic Significance of Methylthioadenosine Phosphorylase Deficiency in Nasopharyngeal Carcinoma. Medicine (Baltimore). 2015; 94:e2271. [PubMed: 26656376]
32. Kryukov GV, Wilson FH, Ruth JR, Paulk J, Tsherniak A, Marlow SE, et al. MTAP deletion confers enhanced dependency on the PRMT5 arginine methyltransferase in cancer cells. Science. 2016; 351:1214–8. [PubMed: 26912360]
33. Marjon K, Cameron MJ, Quang P, Clasquin MF, Mandley E, Kunii K, et al. MTAP Deletions in Cancer Create Vulnerability to Targeting of the MAT2A/PRMT5/RIOK1 Axis. Cell Rep. 2016; 15:574–87. [PubMed: 27068473]
34. Mavrakis KJ, McDonald ER 3rd, Schlabach MR, Billy E, Hoffman GR, deWeck A, et al. Disordered methionine metabolism in MTAP/CDKN2A-deleted cancers leads to dependence on PRMT5. Science. 2016; 351:1208–13. [PubMed: 26912361]
35. Robak P, Robak T. Older and new purine nucleoside analogs for patients with acute leukemias. Cancer Treat Rev. 2013; 39:851–61. [PubMed: 23566572]
36. Lubin M, Lubin A. Selective killing of tumors deficient in methylthioadenosine phosphorylase: a novel strategy. PLoS One. 2009; 4:e5735. [PubMed: 19478948]
37. Tang B, Testa JR, Kruger WD. Increasing the therapeutic index of 5-fluorouracil and 6-thioguanine by targeting loss of MTAP in tumor cells. Cancer Biol Ther. 2012; 13:1082–90. [PubMed: 22825330]
38. Bertino JR, Waud WR, Parker WB, Lubin M. Targeting tumors that lack methylthioadenosine phosphorylase (MTAP) activity: current strategies. Cancer Biol Ther. 2011; 11:627–32. [PubMed: 21301207]
39. Jensen MM, Jorgensen JT, Binderup T, Kjaer A. Tumor volume in subcutaneous mouse xenografts measured by microCT is more accurate and reproducible than determined by 18F-FDG-microPET or external caliper. BMC Med Imaging. 2008; 8:16. [PubMed: 18925932]
40. Hensley H, Quinn BA, Wolf RL, Litwin SL, Mabuchi S, Williams SJ, et al. Magnetic resonance imaging for detection and determination of tumor volume in a genetically engineered mouse model of ovarian cancer. Cancer Biol Ther. 2007; 6:1717–25. [PubMed: 17986851]
41. Lukenbill J, Kalaycio M. Fludarabine: a review of the clear benefits and potential harms. Leuk Res. 2013; 37:986–94. [PubMed: 23787174]
42. Skipper HE, Montgomery JA, Thomson JR, Schabel FM Jr, et al. Structure-activity relationships and cross-resistance observed on evaluation of a series of purine analogs against experimental neoplasms. Cancer Res. 1959; 19:425–37. [PubMed: 13652127]

43. Hill DL, Pittillo RF. Use of Escherichia coli mutants to evaluate purines, purine nucleosides, and analogues. Antimicrob Agents Chemother. 1973; 4:125–32. [PubMed: 4598216]

Significance

Loss of MTAP occurs in about 15% of all human cancers; the MTAP protection strategy presented in this study could be very effective in treating these cancers.

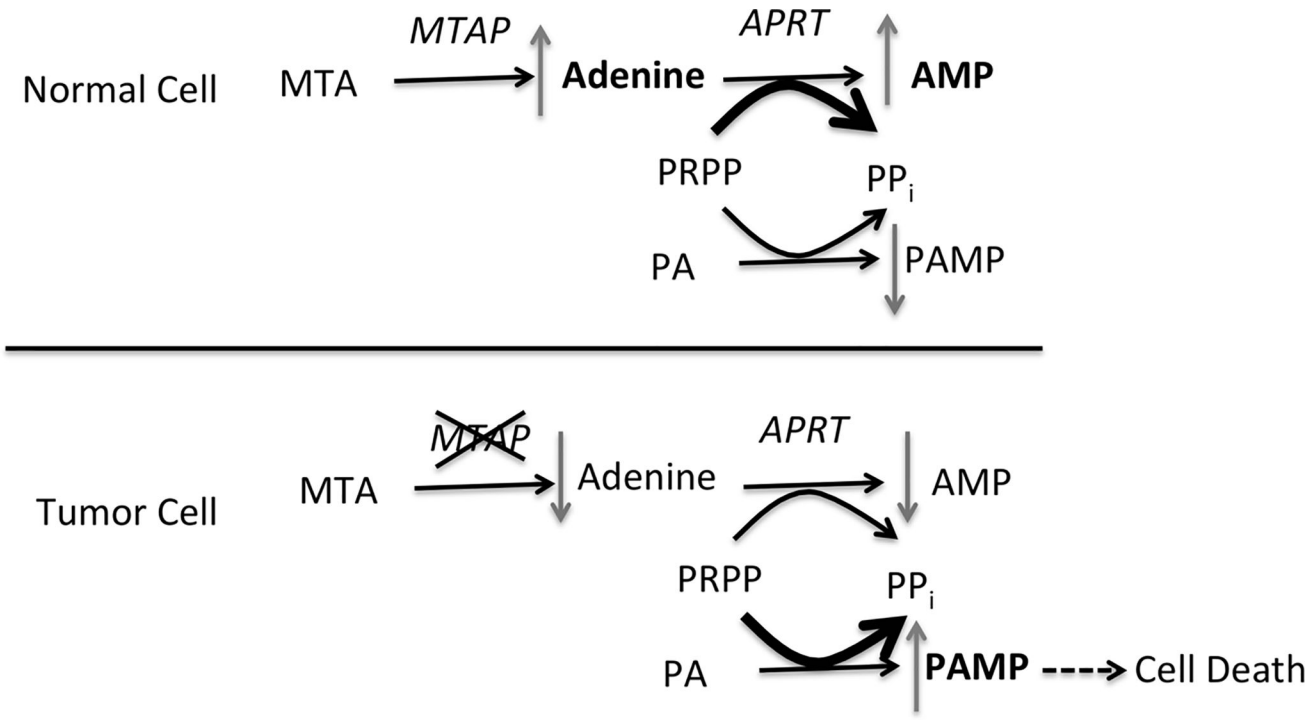

Figure 1.

MTAP protection strategy. In *MTAP*$^{+}$ cells MTA is converted to adenine, which is then used to synthesize AMP by the action of APRT, which transfers the ribose and phosphate from PRPP. Purine analogs (PA) must also be converted to nucleosides (PAMP) by the transfer ribose and phosphate from PRPP (although the exact phosphoribosyltransferase used can vary depending on the analog). High concentrations of MTA inhibit the conversion of PA to PAMP by either competition for PRPP, or competition for APRT. In *MTAP*$^{-}$ cells (bottom), MTA is not converted to adenine, so no competition takes place, resulting in increased production of toxic PAMP.

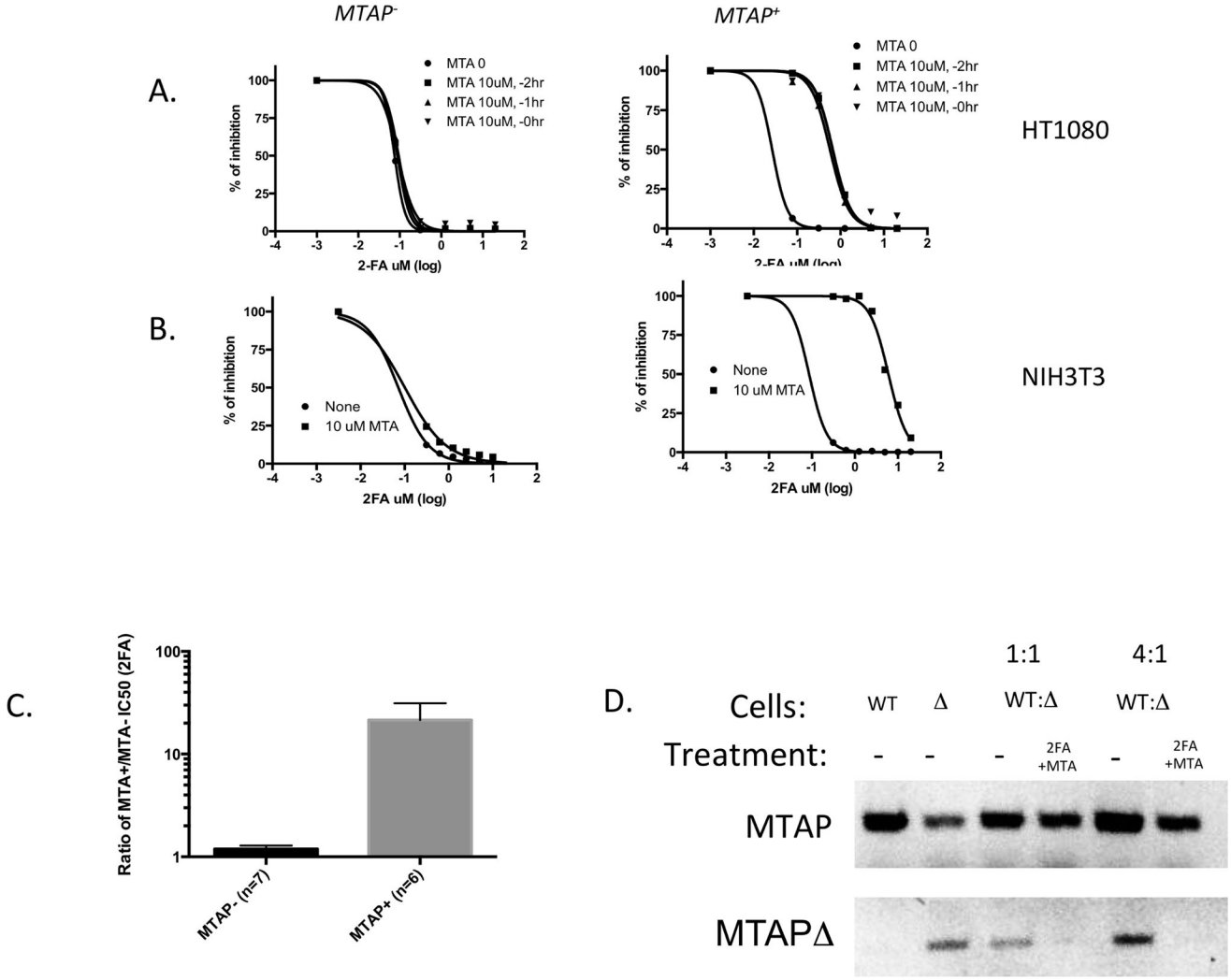

Figure 2.

Effect of MTA on 2FA IC_{50} in isogenic *MTAP*$^{+}$ and *MTAP*$^{-}$ cell lines. **A**, Dose response curve for HT1080:MTAP^{-} and HT1080:MTAP^{+} cell lines treated in the absence or presence on 10 μM MTA. Cells were given MTA either one or two hours before 2FA treatment, or at the same time. **B,** Dose response curves for NIH3T3 mouse fibroblasts that have had *MTAP* deleted by CRISPR technology and non-deleted controls. **C**. Graph shows the ratio of calculated IC_{50} for 2FA either in the presence or absence of 10 μM MTA for 13 different cell lines (Supplementary Table 2). Asterisk indicates P<0.002. **D,** Mixing experiment. DNA gel showing bands from Top row shows PCR product using primers specific for either wild-type MTAP, while bottom row shows PCR product specific toward MTAPΔ allele. DNA from untreated wild-type NIH3T3 cells (WT) or CRISPR MTAPΔ cells are shown in first two lanes (note some WT allele is still present in the CRISPR population). These two cell lines were then mixed in either a 1:1 or 4:1 ratio and treated with 1.25 μM 2FA/10 μM MTA for 70 hours or left untreated and PCR was performed on isolated DNA.

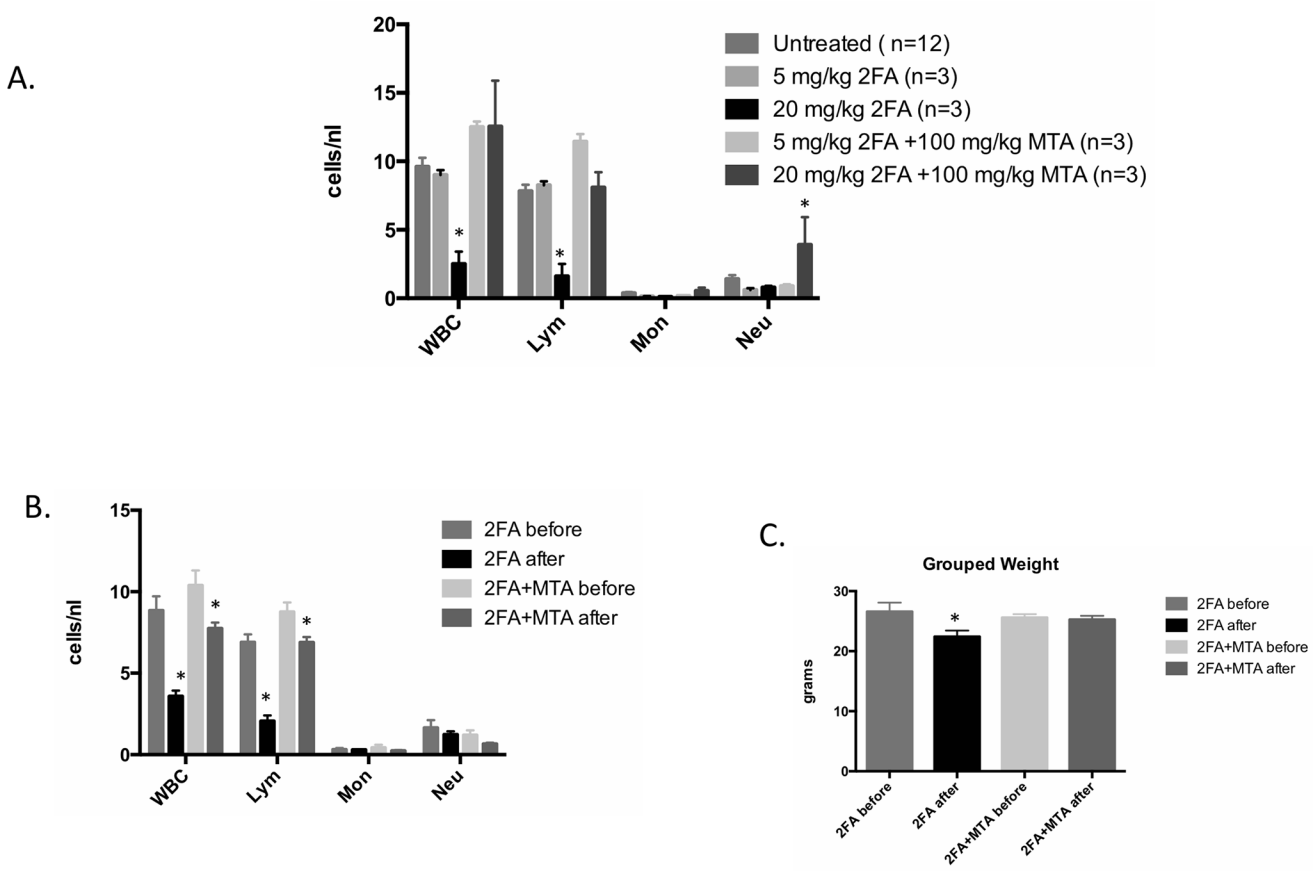

Figure 3.

Effects of 2FA and 2FA+MTA on mouse WBCs. **A,** C57BL6 Mice were given 2FA or 2FA +MTA by IP injection at the indicated dose for five consecutive days once a day for five days and then blood was analyzed eight days after the last injection. SEM is indicated. Asterisk indicates $P<0.05$ compared to untreated control. **B,** Mouse blood was collected at baseline and then C57BL6 mice were given 2FA or 2FA+MTA by IP injection for five consecutive days followed by blood collection four days after last injection. SEM is indicated. Asterisk indicates $P<0.05$ compared to baseline value. **C,** Change in weight for mice in experiment described in B.

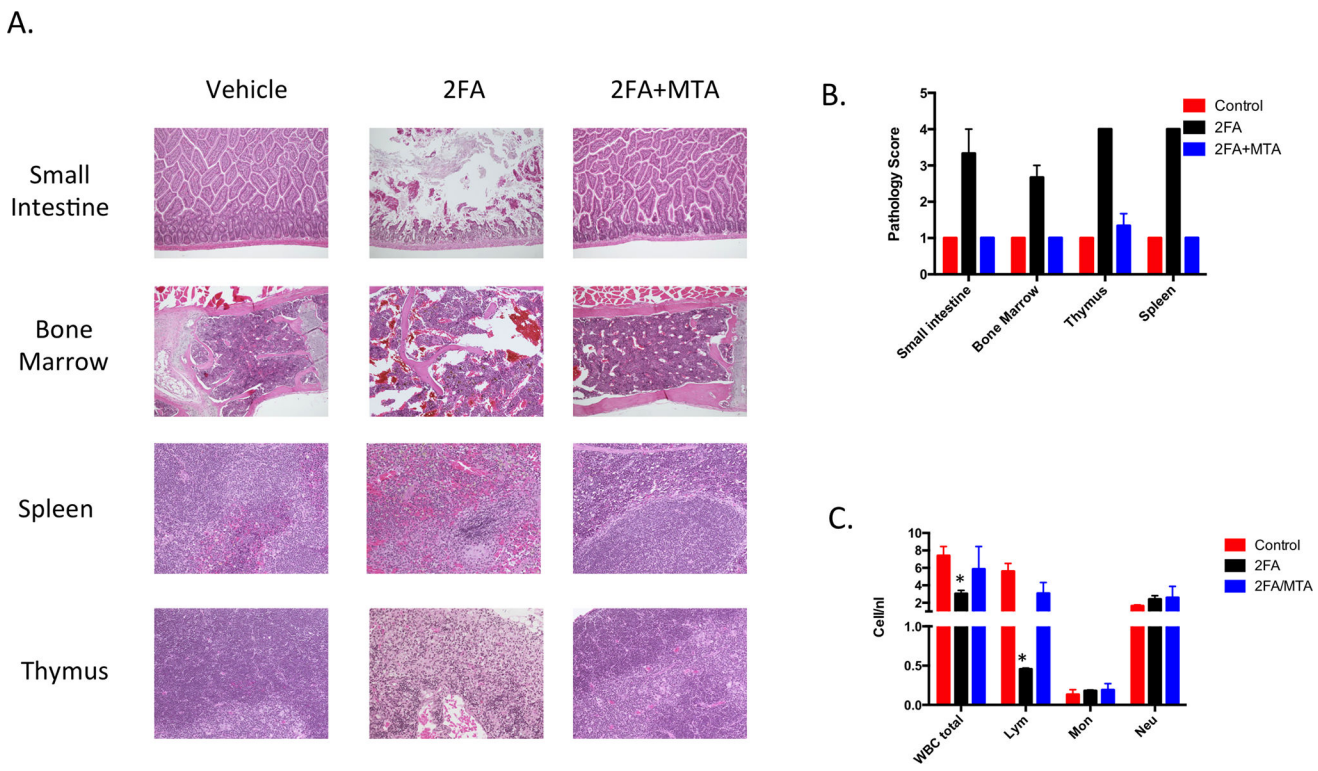

Figure 4.

2FA toxicity in mouse tissues. C57BL6 mice (n=3/group) were injected with either vehicle, 20 mg/kg 2FA, or 20 mg/kg 2FA +100 mg/kg MTA for four consecutive days. Tissue was collected on day 5. **A,** Representative images of indicated H and E stained tissues. **B,** H and E stained images were rated blindly by a pathologist on a four point scale (1=normal; 4=severe cellular atrophy). Mean ratings for each tissue is shown. **C,** Bar chart showing various white blood cell measures in control and treated animals. Error bars show SEM. Asterisk indicates $P<0.05$ compared to untreated control.

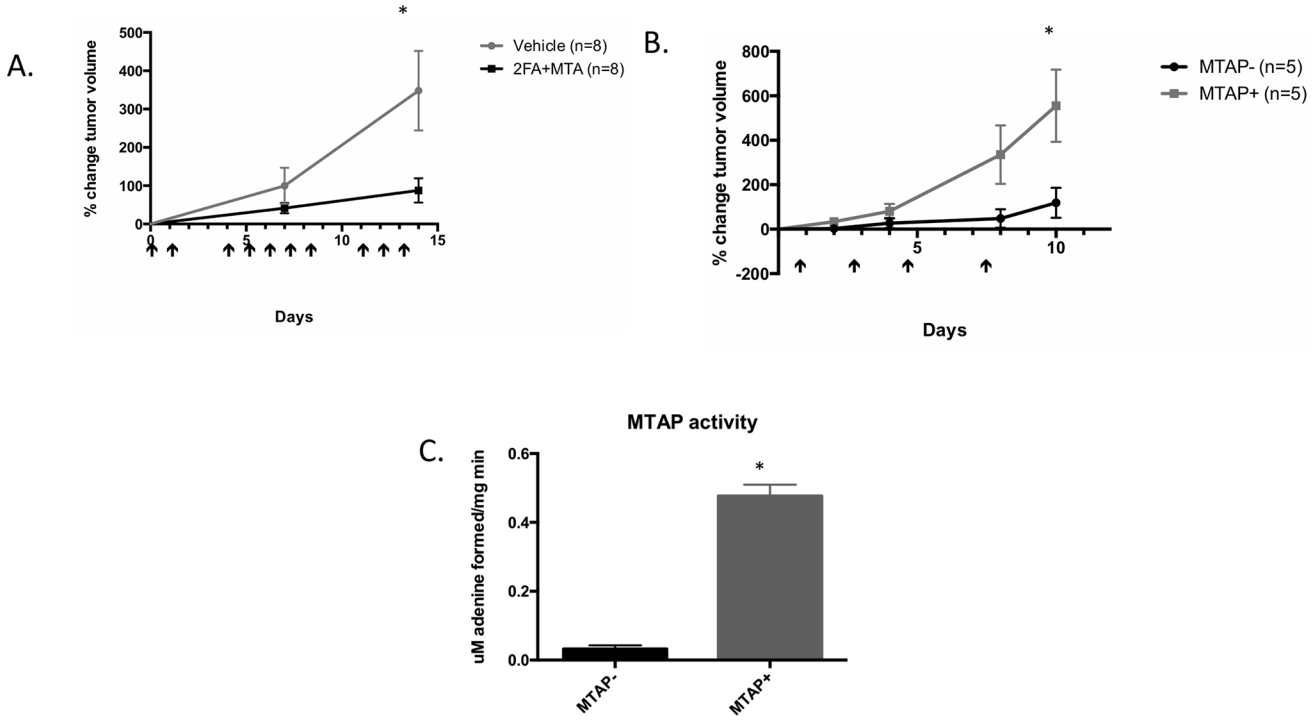

Figure 5.

Effects of 2FA+MTA on HT1080 xenograft tumors. **A,** Comparison of tumor growth in SCID mice injected with *MTAP*$^{-}$ HT1080 cells treated with vehicle and 10 mg/kg 2FA+ 50 mg/kg MTA (n=8 per group). Arrows show days when injected. Error bars show SEM. Asterisk indicates P<0.05 at indicated time. **B,** Comparison of growth rates in *MTAP*$^{-}$ and *MTAP*$^{+}$ HT1080 xenograft tumors treated with 10 mg/kg 2FA+ 50mg/kg MTA (n=5 per group). **C,** Quantification of MTAP activity of tumors isolated at the end of experiment B.

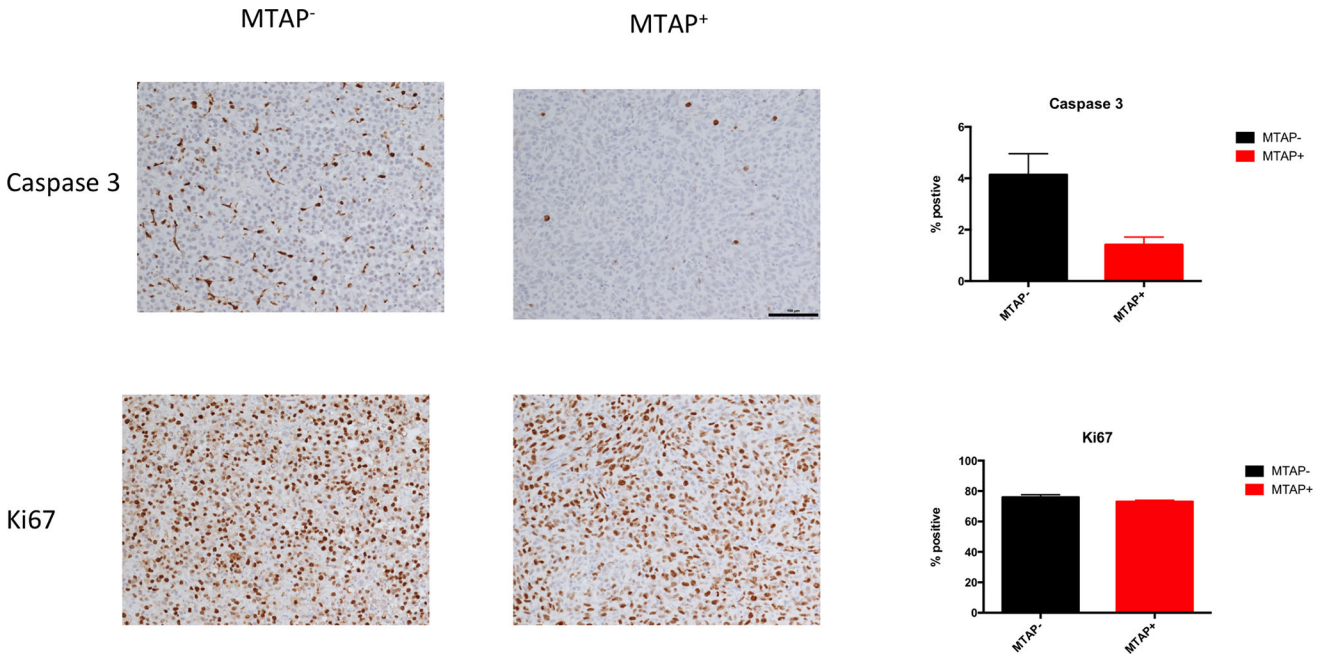

Figure 6.

Caspase 3 and Ki67 stainings of HT1080 *MTAP*$^{+}$ and *MTAP*$^{-}$ xenograft tumors treated with 2FA+MTA (n=5/group). Left side shows representative images of staining for Caspase 3 and KI67 from tumors on indicated genotype. Right side shows quantitation of slides as described in Materials and Methods.

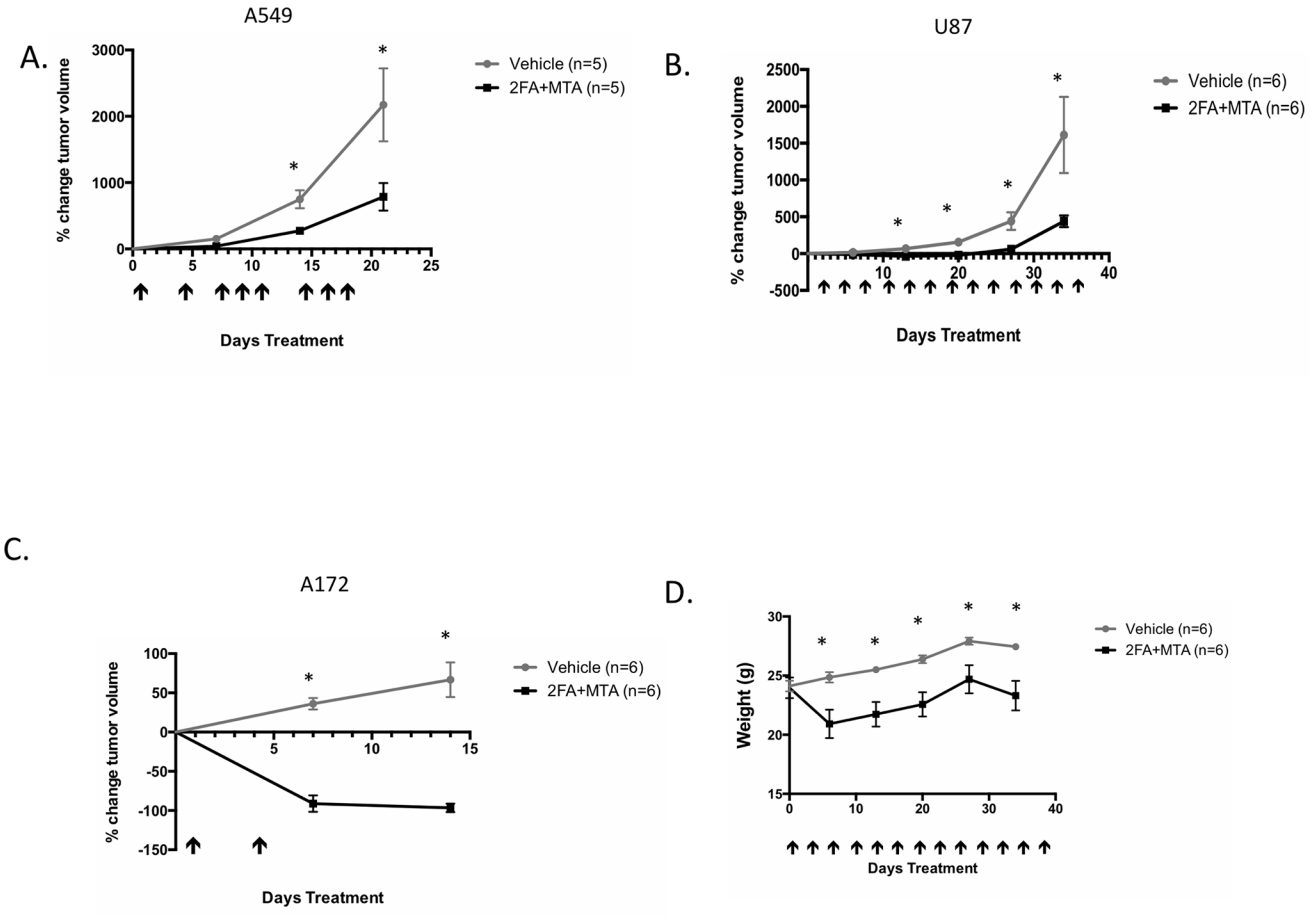

Figure 7.

Effect of 2FA+MTA combination on growth of *MTAP*$^{-}$ U87, A172, and A549 tumor xenografts. **A,** Growth of vehicle treated and 2FA+MTA treated A549 tumors. Days of injection are shown by arrows. Error bars show SEM. Asterisk indicates $P<0.05$ at indicated time. **B,** Growth of treated and untreated U87 tumors. **C,** Growth of treated and untreated A172 tumors. **D,** Weight of mice over time for U87 experiment.